Investigation of Electrostatic Transportation of Lunar Dust Grains due to Ambient Plasma Conditions

Necmi Cihan Örger*, J. Rodrigo Cordova-Alarcon, Kazuhiro Toyoda, Mengu Cho

Laboratory of Spacecraft Environment Interaction Engineering, Kyushu Institute of Technology, 1-1 Sensui-cho, Tobata-ku, Kitakyushu-shi, Fukuoka, Japan 804-8550, p595502j@mail.kyutech.jp, p595903r@mail.kyutech.jp, toyoda@ele.kyutech.ac.jp, cho@ele.kyutech.ac.jp
* Corresponding Author

Abstract

Recent studies have shown that dust grains can be transported in the laboratory experiments due to charging within micro-cavities between the particles [1, 2]. Therefore, electrostatic forces acting on the dust grains can be described as the repulsive Coulomb force between charged grains and the force resulting from the surface electric field due to the plasma sheath above the surface. In this study, we investigate different ambient plasma conditions to understand how the lunar dust particles are mobilized under the variation of surface potential, dust potential, electric field and the plasma sheath above the lunar terminator. In addition, electrostatic forces are compared to the gravity force and the contact forces for the micron and submicron sized dust particles, and it has been seen that the repulsive force between the charged dust grains can be stronger than the other forces. Finally, the current level of the experimental work is presented, which is prior to investigation of the impact modification on the electrostatic lofting of the silica dust grains in the vacuum chamber.

Keywords: Lunar dust, lunar surface charging, dust lofting, solar wind, ambient plasma.

1. Introduction

The lunar surface directly interacts with the ambient plasma and solar irradiation in the absence of a global magnetic field and a dense atmosphere. Therefore, it is charged to various surface potentials depending on the surrounding plasma conditions in the vicinity of the Moon and the photoemission of electrons from the dayside surface. The recent orbital measurements and simulation studies have shown that the surface potential is highly variable depending on the location on the Moon from dayside to night side region [3-10].

Surveyor missions observed the lunar horizon glow (LHG) on the western horizon in 1966 and 1968, and these observations suggested that the dust particles with ~5-6 μm radius were reaching up to approximately 0.3 meter above the surface near the lunar terminator [11].

The Lunar Atmosphere and Dust Environment Explorer LADEE mission measured the dust particles between 20-100 km altitudes around the Moon, and the results concluded that the dust densities suggested by the LHG observations during the Apollo 15 orbit sequences were not present [12]. In addition, LRO (Lunar Reconnaissance Orbiter) The Lyman-Alpha Mapping Project (LAMP) UV spectrograph measurements could not measure any distinguishable dust densities suggesting any excessive brightness [13]. In both measurements, the solar wind conditions were unremarkable; however, the annual meteor showers were present. The difference between the measured dust populations requires further investigation.

In this paper, we investigate the lofting of the dust particles by the electrostatic forces due to the surface electric field and the charging within the micro-cavities between dust particles. First, we calculate the minimum charge required by a dust particle in order to leave the surface. Second, the maximum height that a dust particle can reach after launched vertically is presented. Finally, we shortly discuss the current level of the vacuum chamber experiments in our laboratory.

2. Lunar Surface Charging

The current balance approach has been used to calculate the terminator region surface potential, electric field and Debye sheath thickness.

The following assumptions are applied to the model for simplification such as:
- The Moon is a perfect sphere.
- The interaction with the current sources is in the equilibrium state.
- The lunar surface material conductivity is almost zero.
- Plasma sheath is collisionless.
- The secondary electron temperature is taken as 2.5 eV [14].
- Plasma population in the vicinity of the Moon has Maxwellian velocity distribution.
- All ions are protons, and the plasma has no magnetic field.
- Potential distributions in the plasma sheath are monotonic.

In steady state, the net equilibrium current to the surface at the lunar terminator can be given as:

$$J_i + J_e + J_{sec} = 0 \qquad (1)$$

The elements of Eq.1 can be described as ion current J_i to the surface, electron collection current from surrounding plasma J_e and the secondary electron emission J_{sec} from the surface.

3. Electrostatic Dust Lofting

3.1 Dust Charging

Recent laboratory experiments have shown that dust grains can be lofted from the surface due to charging within micro-cavities between the particles by the photoemission of electrons or the secondary electron emission (Fig. 1), and a patched dust charging model has been suggested as [1, 2]:

$$Q_r = -0.5\eta \, C \, T_{ee} \tag{2}$$

For a single dust particle resting on the lunar surface; the force equilibrium can be given as:

$$F_c + F_{Coulomb} + F_{gravity} + F_{EF} = 0 \tag{3}$$

F_c is the contact forces between the dust grain surfaces whereas $F_{Coulomb}$ is the repulsive force between the dust grains due to charge accumulation within micro-cavities. In addition, $F_{gravity}$ is the gravity force, and F_{EF} is the electrostatic force due to surface electric field.
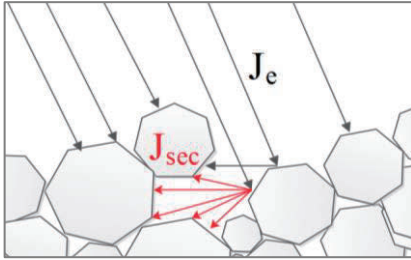
Fig. 1. Dust charging within the micro-cavities.

To release a particle from the lunar terminator, the following condition must be met as below:

$$F_{Coulomb} + F_{EF} > F_c + F_{gravity} \tag{4}$$

We can find the minimum value of the factor η as:

$$\eta > \frac{2a}{T_{ee}} \sqrt{\frac{2CS^2}{\pi a \varepsilon_0} + \frac{4a\rho_{dust}g_{Lunar}}{3\varepsilon_0} - 2E_0^2} \tag{5}$$

Depending on the size of the particle radius a, the surface electric field E_0 and the lunar gravity acceleration g_{Lunar} can have significant influence on the electrostatic particle transportation. In conclusion, a dust particle will not leave the surface until the particle can collect sufficient charge within the micro-cavity or an external force is applied.

3.2 Maximum Height Calculation

Initial velocity v_o that a separated particle can reach by assuming that all the electrostatic energy transforms into kinetic energy can be estimated as:

$$0.5 \, m_{dust} v_o^2 = \sum E_{ES} - \sum W \tag{6}$$

It is estimated as the sum of the energy from the electrostatic repulsion from the surface E_{ES} and the work done against gravity and contact forces W.

$$v_{ox}^2 + v_{oy}^2 + v_{oz}^2 = \frac{2}{m_{dust}} \left[\sum E_{ES} - \sum W \right] \tag{7}$$

$$v_{oz} = \left[\frac{2}{m_{dust}} \left(\frac{Q_r^2}{8\pi\varepsilon_0 a} + (2\pi a^2 \varepsilon_0 E_0^2 - m_{dust}g_{Lunar})d_1 \right. \right. \\ \left. \left. - CS^2 (2a)d_2 \right]^{0.5} \tag{8}$$

For the maximum height calculation, v_{ox} and v_{oy} are assumed as 0 (Eq. 8). In the experiments, the silica dust grains were launched from the surface with variety of angles; however, the vertical launch will achieve the maximum dust height in this case.

d_1 is the approximate distance for electrostatic potential energy to transform into kinetic energy. For micron and submicron sized grains, it has been seen that $h_{max} \gg d_1$ and $\lambda_D \gg d_1$. d_2 is the separation distance from the contact forces, and it has been suggested as several dozens of nanometers to cancel the contact forces for a dust particle [15].
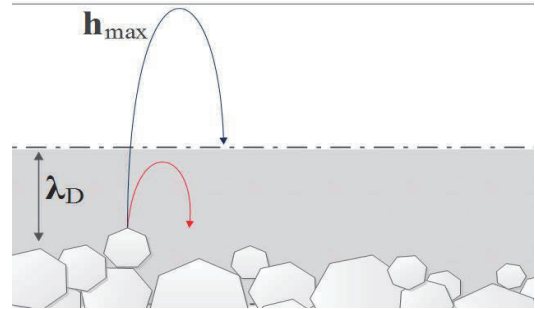
Fig. 2. Lofting dust grains.

Depending on the electrostatic acceleration and the lunar gravity, the dust particles can have different behaviors within the electron sheath above the lunar terminator. These conditions can be explained as below:

- **Condition 01:** $a_{dust} = \frac{Q_{dust}}{m_{dust}} E_0 - g_{Lunar} > 0$

Dust particles accelerate within the electron sheath; therefore, they have a higher exit velocity than the initial vertical velocity.

- **Condition 02:** $a_{dust} = \frac{Q_{dust}}{m_{dust}} E_0 - g_{Lunar} < 0$

Some of the decelerating dust particles have lower heights than Debye length or they leave the electron sheath with lower velocities than the initial vertical velocity. Therefore, they can be expressed as:

1. Dust particles leaving the electron sheath after decelerating ($h_{max} > \lambda_D$).
2. Dust particles reaching zero velocity within the sheath ($h_{max} \leq \lambda_D$).

- **Condition 03:** $a_{dust} = \frac{Q_{dust}}{m_{dust}} E_0 - g_{Lunar} = 0$

Dust particles move with constant speed until leaving the electron sheath.

3.3 Simulation Results

For the simulations, we used the plasma conditions we have investigated previously for the terminator surface charging [16, 17]. These results had been used together with the dynamic fountain model of lunar dust [18]; however, the calculations are remade since the charging mechanism has been changed.

Table 1: Simulation Inputs for Different Conditions.

Condition	n_0 (cm^{-3})	T_e (eV)	T_i (eV)	V_{SW} (km/sec)
Slow Stream SW	10.0	12.1	8.6	400
Fast Stream SW	5.0	12.1	12.9	650
CME Post-shock 01	20.0	14.8	43.0	600
Early-CME 01	3.0	6.6	6.8	650
Late-CME 01	50.0	3.2	2.6	500
CME Post-shock 02	51.0	9.1	43	560
Early-CME 02	0.4	4.0	1.2	450
Late-CME 02	43.4	3.1	1.0	390
CME Post-shock 03	25.0	32.1	61.9	710
Early-CME 03	3.0	3.0	0.44	465
Late-CME 03	11.4	8.5	14.3	455

Table 2: Maximum dust heights in meter for dust particles with 0.1, 1 and 5 μm radius.

Condition	Dust Particle Radius		
	0.1 μm	1 μm	5 μm
Slow Stream SW	204.538	5.488	0.310
Fast Stream SW	194.609	2.859	0.303
CME Post-shock 01	204.681	7.472	0.317
Early-CME 01	112.995	2.022	0.297
Late-CME 01	63.496	3.015	0.313
CME Post-shock 02	122.366	4.873	0.321
Early-CME 02	83.917	1.599	0.292
Late-CME 02	67.710	3.148	0.314
CME Post-shock 03	453.499	15.327	0.340
Early-CME 03	70.730	1.910	0.296
Late-CME 03	133.057	3.500	0.306

The value η in Eq.2 has been calculated as approximately 5.8, 18.4 and 41.1 for 0.1, 1 and 5 μm radius dust grains respectively. In addition, the maximum value of the initial vertical velocity has been found as 6.670 m/sec, 2.158 m/sec and 0.964 m/sec for 0.1, 1 and 5 μm radius dust grains. It is seen that the enhanced charging number η increases with the particle size whereas the initial vertical speed after the separation decreases. For the maximum dust heights calculations, it has been seen that only the third CME post-shock condition was able to loft the submicron size dust grains up to approximately 450 meter. This is due to higher electron temperature together with plasma density as 25 cm^{-3} since the electron temperature enhances the surface electric field while the Debye sheath thickness allows particles to accelerate within a sufficient distance. According to the results, the particles with 5 μm radius are able to reach up to approximately 29-34 cm heights in various ambient plasma conditions, which is in agreement with the upper limit of Surveyor observations (Table 2).

3.4 Laboratory Experiments
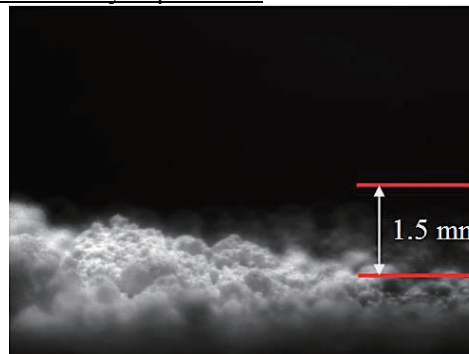
Fig. 3. Silica dust particles.

Previous experiments have shown that the secondary electron emission is a critical mechanism for the electrostatically lofted dust particles, and initial vertical speed of dust particles was reported together with estimated charging value of η [1,2]. We use irregular shape silica dust grains with 0.15 μm median size on a graphite plate while observing with the microscopic telescope in our experiments.

Fig. 4. Silica dust lofting under the electron beam.

Some of the particles leaving the surface under the electron beam were carrying smaller particles on their surfaces in some cases. Kapton tape was put in a distance of ~5-10 cm from the dust pound with the adhesive surface on the top, and this was monitored under the microscope at the end of each experiment. It was seen that single particles were collected by the adhesive surface of Kapton tape while clumps of dust were observed closer to the dust pound.

6. Conclusions

In this study, various plasma conditions are investigated in order to estimate the maximum dust heights, initial vertical speed in the electron sheath and the required charging number η above the terminator region. It has been found that particles with 5 μm radius can reach the similar heights suggested by LHG observations. In addition, it has been seen that the maximum heights of the smaller particles are more subjected to the influence of the ambient plasma conditions (Table 2).

Laboratory experiments have demonstrated the lofting of the silica dust particles under the electron beam similar to the previous experimental results [1, 2]. In addition, single particles were launched from the surface as well as the clumps of the dust grains. Future work will focus on the particle separation from the surface and the behavior of the dust particles after separation under the electron beam with the impact modification of dust launching from the surface.

References

[1] Wang, X., Schwan, J., Hsu, H. W., Grün, E., & Horányi, M. (2016). Dust charging and transport on airless planetary bodies. *Geophysical Research Letters*, *43*(12), 6103-6110.

[2] Schwan, J., Wang, X., Hsu, H. W., Grün, E., & Horányi, M. (2017). The charge state of electrostatically transported dust on regolith surfaces. *Geophysical Research Letters*, *44*(7), 3059-3065.

[3] Manka, R. H. (1973). Plasma and potential at the lunar surface. *Photon and Particle Interactions with Surfaces in Space* (pp. 347-361). Springer Netherlands.

[4] Walbridge, E. W. (1969). On "Photoelectric screening of bodies in interplanetary space" by Singer and Walker. *Icarus*, *10*(2), 342-343.

[5] Freeman, J. W., & Ibrahim, M. (1975). Lunar electric fields, surface potential and associated plasma sheaths. *Earth, Moon, and Planets*, *14*(1), 103-114.

[6] Stubbs, T. J., Farrell, W. M., Halekas, J. S., Burchill, J. K., Collier, M. R., Zimmerman, M. I., ... & Pfaff, R. F. (2014). Dependence of lunar surface charging on solar wind plasma conditions and solar irradiation. *Planetary and Space Science*, *90*, 10-27.

[7] Farrell, W. M., Poppe, A. R., Zimmerman, M. I., Halekas, J. S., Delory, G. T., & Killen, R. M. (2013). The lunar photoelectron sheath: A change in trapping efficiency during a solar storm. *Journal of Geophysical Research: Planets*, *118*(5), 1114-1122.

[8] Halekas, J. S., Delory, G. T., Lin, R. P., Stubbs, T. J., & Farrell, W. M. (2009). Lunar surface charging during solar energetic particle events: Measurement and prediction. *Journal of Geophysical Research: Space Physics*, *114*(A5).

[9] Halekas, J. S., Delory, G. T., Brain, D. A., Lin, R. P., Fillingim, M. O., Lee, C. O., ... & Hudson, M. K. (2007). Extreme lunar surface charging during solar energetic particle events. *Geophysical research letters*, *34*(2).

[10] Halekas, J. S., Delory, G. T., Lin, R. P., Stubbs, T. J., & Farrell, W. M. (2008). Lunar Prospector observations of the electrostatic potential of the lunar surface and its response to incident currents. *Journal of Geophysical Research: Space Physics*, *113*(A9).

[11] Rennilson, J. J., & Criswell, D. R. (1974). Surveyor observations of lunar horizon-glow. *The Moon*, *10*(2), 121-142.

[12] Horányi, M., Szalay, J. R., Kempf, S., Schmidt, J., Grün, E., Srama, R., & Sternovsky, Z. (2015). A permanent, asymmetric dust cloud around the Moon. *Nature*, *522*(7556), 324-326.

[13] Grava, C., Stubbs, T. J., Glenar, D. A., Retherford, K. D., & Kaufmann, D. E. (2017). Absence of a detectable lunar nanodust exosphere during a search with LRO's LAMP UV imaging spectrograph. *Geophysical Research Letters*.

[14] Vaverka, J., Richterová, I., Pavlu, J., Šafránková, J., & Němeček, Z. (2016). Lunar surface and dust grain potentials during the earth's magnetosphere crossing. *The Astrophysical Journal*, *825*(2), 133.

[15] Popel, S. I., Lisin, E. A., Izvekova, Y. N., Atamaniuk, B., Dolnikov, G. G., Zakharov, A. V., & Zelenyi, L. M. (2016). Meteoroid impacts and dust particles in near-surface lunar exosphere. *Journal of Physics: Conference Series* (Vol. 774, No. 1, p. 012175).

[16] Orger, N. C., Cordova-Alarcon, J. R., Toyoda, K., and Cho, M. (2017). Lunar Surface Charging and Electrostatic Lofting of Lunar Dust Particles under Different Solar Wind Conditions and Solar Ultraviolet Radiation. *JAXA Special Publication: Proceeding of the 13th Spacecraft Environment Symposium 宇宙航空研究開発機構特別資料: 第13回「宇宙環境シンポジウム」講演論文集* (p. 81).

[17] Orger, N. C., Cordova-Alarcon, J. R., Toyoda, K., and Cho, M. (2017). Simulation of Lunar Surface Charging, Electric Field and Dust Lofting with Attitude Control of a CubeSat Mission. Joint Conference: 31st ISTS , 26th ISSFD & 8th NSAT.

[18] Stubbs, T. J., Vondrak, R. R., and Farrell, W. M. (2006). A dynamic fountain model for lunar dust. *Advances in Space Research*, *37*(1), 59-66.